Nano-Structures & Nano-Objects 15 (2018) 28–39

Contents lists available at ScienceDirect

Nano-Structures & Nano-Objects

journal homepage: www.elsevier.com/locate/nanoso

Investigation on the morphology and optical properties of self-assembled Ag Nanostructures on *c*-plane GaN by the control of annealing temperature and duration

Mao Sui [a], Sundar Kunwar [a], Puran Pandey [a], Quanzhen Zhang [a], Ming-Yu Li [a], Jihoon Lee [a,b,*]

[a] College of Electronics and Information, Kwangwoon University, Nowon-gu Seoul 01897, South Korea
[b] Institute of Nanoscale Science and Engineering, University of Arkansas, Fayetteville AR 72701, USA

HIGHLIGHTS

- Various configuration, size and density of Ag nanostructures demonstrated by the control of annealing temperature and duration via the solid state dewetting.
- Demonstration of a clear shift in the growth regimes of Ag nanostructures depending upon the initial Ag film thickness.
- Dipolar resonance peak demonstrated a clear distinct peak shift along with the evolution of Ag nanostructures.

GRAPHICAL ABSTRACT

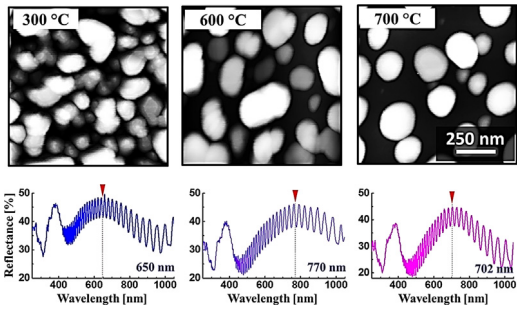

ARTICLE INFO

Article history:
Received 29 October 2017
Received in revised form 22 January 2018
Accepted 5 March 2018

Keywords:
Ag nanostructures
c-plane GaN
Localized surface plasmon resonance
Solid-state-dewetting
Growth regimes

ABSTRACT

In this paper, the systematic control of self-assembled Ag nanostructures (NSs) on *c*-plane GaN is demonstrated by the control of annealing temperature (AT) and annealing duration (AD) at diverse Ag film thicknesses based on the solid-state-dewetting. The Ag NSs evolve in four distinctive growth regimes in terms of size, density and configuration with the 10 nm initial film thickness such as (i) nano-voids and -mounds (ii) nanoclusters (iii) nanoparticles (NPs) and (iv) NPs with sublimation. However, only three growth regimes are observed with the 40 nm set with variant NSs morphology due to the suppression of dewetting and diffusion. Meanwhile, based on the AD control with 30 nm Ag film, the size of Ag NSs are exponentially decreased in terms of the RMS roughness (Rq) and surface area ratio (SAR) due to the extensive sublimation of Ag atoms. The formation of various Ag NSs is discussed based on the Volmer–Weber growth model under the influence of several diffusion condition and Ag sublimation. The optical properties of Ag NSs are studied by the reflectance, Raman and photoluminescence, and the spectral evolution including the peak intensity and shift are discussed in terms of the specific plasmon resonance absorption band and surface tensile strain in reference to the morphology evolution of Ag NSs. In specific, the dipolar resonance peak clearly demonstrates shifts depending on the evolution of Ag NSs.

1. Introduction

Metallic NSs (MNSs) can play important roles as crucial components in various applications and their properties and applicability are strongly dependent on the size, configuration, density as well

* Corresponding author at: College of Electronics and Information, Kwangwoon University, Nowon-gu Seoul 01897, South Korea.
E-mail address: jihoonlee@kw.ac.kr (J. Lee).

https://doi.org/10.1016/j.nanoso.2018.03.006
2352-507X/

as distance between them. [1–5]. In particular, the photo-excited MNSs can trigger selective spectral absorption and enhanced electromagnetic field due to the localized surface plasmon resonance (LSPR), which endows the MNSs great potentials to be applied in various optoelectronic devices and their performances may exceed the conventional [6–12]. For instance, due to the strong coupling between multiple quantum wells and MNSs, an output enhancement of ∼30% has been reported for the InGaN/GaN blue LED. [9] Also, the MNSs open up a promising route to improve the efficiency of biosynthesis, photovoltaic devices, catalysis, and photocatalytic water splitting as the hot electrons generated during the decay of surface plasmon can escape and be collected [10–15]. Among various MNSs, the Ag NSs exhibit active LSPR absorption band in the visible region and the LSPR properties can be directly modulated by the control of size, density, spacing and configuration [1]. On the other hand, GaN, as one of the most widely utilized wide bandgap semiconductors, has been extensively adapted in various high-power and high-efficiency optoelectronic devices [16–18]. Furthermore, embedding the Ag NSs on GaN can demonstrate significantly enhanced performance of GaN-based LEDs due to the resonance coupling between the NSs and quantum wells [19]. Therefore, the study on the morphological and optical evolution of various Ag NSs on GaN can offer an essential reference for the corresponding applications based on the Ag/GaN. However, the systematic study based on the control of annealing temperature and duration has been rarely reported up to date. Thus, in this work, the self-assembled Ag NSs are investigated on *c*-plane GaN in terms of the morphology and optical evolution. Various configuration, size and density of Ag NSs are demonstrated depending up on the annealing temperature and duration. The temperature dependent evolution of various Ag nanostructures is discussed based on the Volmer–Weber growth model, surface diffusion and sublimation of Ag atoms. In particular, with a relatively thinner Ag thickness of 10 nm, four distinctive growth regimes of Ag NSs, such as (i) nano-voids and -mounds, (ii) nanoclusters, (iii) NPs and (iv) size reduction of NPs, are observed along with the annealing temperature control. Meanwhile, with 40 nm Ag thickness, only three growth regimes of Ag nanostructures are observed as the dewetting of Ag films is suppressed. On the other hand, by the control of the annealing duration, the gradual evolution of configuration and reduction of NSs size is demonstrated at a constant annealing temperature 700 °C and Ag film thickness of 30 nm. The evolution of Ag NSs in the annealing duration set can be due to the concurrent influence of surface diffusion, Ostwald's ripening and Ag sublimation. Furthermore, morphological dependent optical properties of Ag NSs are investigated by the reflectance, Raman and photoluminescence. In particular, the LSPR active wavelength induced by the Ag NSs morphology control reveals a gradual shift within the wavelength between 550 and 950 nm.

2. Experimental section

In this work, Ag NSs (NSs) were fabricated on ∼5 μm epi-ready n-type GaN template on *c*-plane sapphire (PAM-XIAMEN Co. Ltd, China). To begin with, the substrates were diced into 6 × 6 mm^2 squares and treated with a thermal degassing at 350 °C for 30 min under the vacuum below 1.0 × 10^{-4} Torr to remove the oxides, trapped gases as well as various particulates. The AFM top-views of bare GaN after the degassing is shown in Fig. 1(a). Fig. S1 shows the corresponding photoluminescence (PL) spectrum with the PL peak at 363.44 nm (corresponding to 3.41 eV) by a 266 nm laser excitation and Raman spectrum with the E_2 peak at 569 cm^{-1} and A_1 peak at 735.4 cm^{-1}, excited by 532 nm laser. Subsequently, Ag films were deposited by a sputtering in a plasma ion-coater with a deposition rate of 0.1 nm/s under the chamber vacuum below 1.0 × 10^{-1} Torr at an ambient temperature. To investigate the temperature effect, 2 sets of samples were prepared such as 10 and 40 nm, and a 30 nm set was prepared for the annealing duration effect control. Figs. 1(b)–1(f) show the AFM top-views, line-profiles and corresponding surface roughness (Rq) and surface area ratio (SAR) plots of the as-deposited samples before annealing. With the thicker films, Ag agglomerates were observed, i.e. with 30 and 40 nm. The Rq and SAR of as-deposited samples were gradually increased along with the increased Ag thickness. Then, the as-deposited samples were mounted on an Inconel holder and transferred into a pulsed laser deposition system in which the annealing process was executed. Precisely controlled by the programmed recipes, the samples were heated from the ambient temperature to the target with a fixed ramp rate of 4 °C s^{-1} under the chamber vacuum below 1.0 × 10^{-4} Torr. The annealing temperature was systematically varied between 150 and 700 °C with an identical annealing duration of 60 s for the two annealing temperature sets. For the annealing duration set, the AD was varied between 0 and 3600 s with the temperature fixed at 700 °C. Immediately after each growth, the temperature was cooled down to the ambient to prevent the undesired ripening effect. All procedures for the annealing was computer controlled and other manual procedures were strictly kept at constant for the consistency between the samples. The morphology of Ag NSs was characterized by an atomic force microscope (AFM) (XE-70, Park Systems, South Korea) and scanning electron microscope (SEM) (CX-200, COXEM, South Korea). The AFM probes utilized were NSC16/AIBS and operated in a non-contact mode. The probes possessed a length of 125 μm, width of 30 μm and thickness of 4 μm. The XEI software was used to obtain the processed morphological data including top- and side-views, line-profiles, Rq and SAR, etc. An energy-dispersive X-ray spectroscope (Noran System 7, Thermo Fisher, USA) was employed for the surface elemental characterization. The reflectance, Raman and photoluminescence spectra of samples were obtained at room temperature by a UNIRAM II system equipped with a charge coupled device (CCD) detector. (UniNanoTech, South Korea). Halogen lamp (450 nm ≤ wavelength ≤ 1050 nm) and deuterium lamp (250 nm ≤ wavelength ≤ 450 nm) were utilized as light sources in the reflectance. An excitation laser of 532 nm was used for the Raman with the power of 220 mW whereas the photoluminescence was excited by a pulsed laser of 266 nm with 3.5 mW.

3. Results and discussion

3.1. Morphological evolution of Ag NSs (NSs) with 10 nm thick film

Fig. 2 shows the overview of Ag nanostructure (NS) evolution on *c*-plane GaN with the Ag thickness of 10 nm by the variation of annealing temperature (AT) between 150 and 700 °C for 60 s. Generally, the Ag NSs evolved in four distinctive growth regimes along with the increased AT: (i) nano-voids and -mounds (150 ≤ AT ≤ 250 °C), (ii) nanoclusters (250 < AT ≤ 400 °C), (iii) NPs (400 < AT ≤ 600 °C) and (iv) decreased NPs (600 °C <AT). The AFM side-views of representing NSs and their line-profiles of four distinctive regimes are shown in Fig. 3 and magnified AFM top-views are exhibited in Fig. S2. To being with, the evolution of Ag NSs in the growth regime (i) can be discussed based on the solid-state-dewetting (SSD) process [20]. A metallic film deposited by a sputtering at an ambient is usually metastable due to the presence of crystalline imperfections such as atomic vacancies, defects and grains. At the same time, the surface reactivity, crystallinity and defects of the GaN surface can significantly affect the dewetting of the Ag films. In addition, the adhesive energy of Ag on substrate surface is very weak [21], which can result in the enhanced surface diffusion of Ag adatoms on GaN during annealing. Along with the thermal energy supplied, the film undergoes the SSD such that the adatoms diffuse and find their atomic sites, resulting in the